CHAPTER 4 RESULTS AND DISCUSSION

The experimental results in previous chapter will be discussed here. The discussion outlines the processes of this research work from resulting of effect of thermal heating on film structure, chemical bonding, wear resistance, corrosion resistance, optical property, film density, surface roughness.

4.1 Effect of thermal heating on film structure

This section presents the effect of thermal heating on film structure characterized by Raman spectroscopy.

Raman is widely used as a non-destructive method to characterize the structural quality of carbons [14]. This method can distinguish the bonding type, domain size, and sensitivity to internal stress in amorphous and nanocrystalline carbon films. Raman spectra are usually discussed in the context of short distance ordered sp^3 and sp^2 bonds [14-16]. To analyze the Raman spectra quantitatively, Raman spectra are fitted to two Guassian peaks which defined as the disorder (D) and graphite (G) peaks. Previous studies have shown that the shift of G and D peaks and the change of D peak intensity in Raman spectra can explain the information about the DLC films structure [16-17].

Raman spectra shown in Figure 4.1 exhibit an overall pattern of the as-deposited ta-DLC films and the annealed films at different temperatures and times. The shift of the Raman spectra of DLC films to higher wavenumber with increasing temperature can be observed. The experimental data obtained above show that the effect of annealing temperature on the ta-DLC films can be divided into two stages. At first stage up to 200 ºC, there is only slight change in film structure. At second stage at 300 ºC, the structure is significantly changed as shown in Raman spectra.

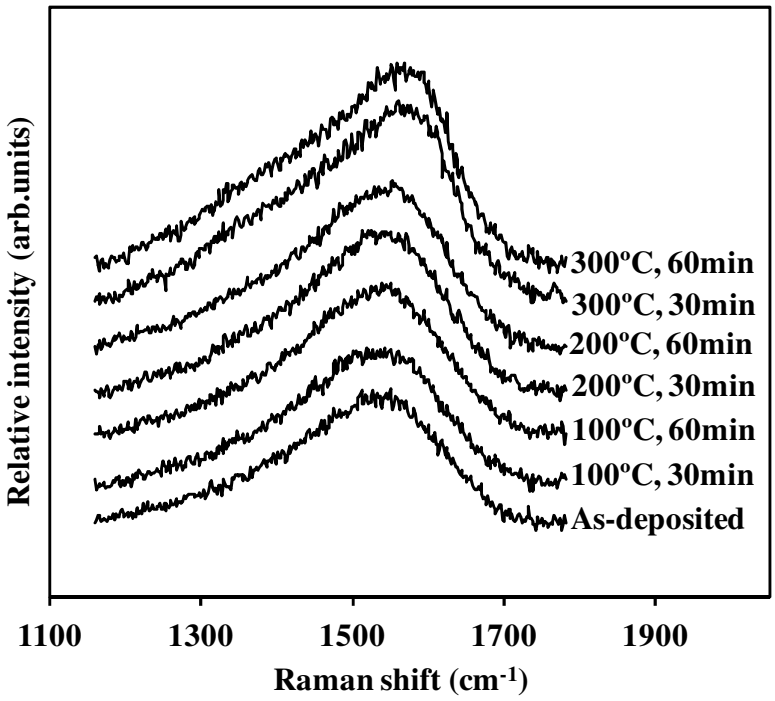

Figure 4.1 Raman spectra of the as-deposited ta-DLC films and the annealed films at different temperatures and times.

Table 4.1 Raman parameters of the as-deposited ta-DLC and the annealed films at different temperatures and times

Temp (ºC)	Time (min)	Position of D peak (cm^{-1})	Intensity of D peak (count)	FWHM of D peak (cm^{-1})	Position of G peak (cm^{-1})	Intensity of G peak (count)	FWHM of G peak (cm^{-1})	I_D/I_G
25	0	1439	385	252	1551	168	620	0.537
100	30	1437	382	252	1553	171	657	0.584
100	60	1440	437	251	1555	169	717	0.614
200	30	1442	491	251	1559	164	768	0.639
200	60	1443	507	254	1561	163	771	0.658
300	30	1458	778	266	1579	130	885	0.881
300	60	1458	804	268.	1581	128	885	0.910

Figure 4.2 (a-b) shows the change of D peak and G peak as function of annealing temperatures and times. The D and G peak of as-deposited ta-DLC film was located at 1439 cm^{-1} and 1554 cm^{-1}, respectively. After annealing, both peaks shifted to higher wavenumber. Maximum shift was observed at the highest annealing temperature of 300 ºC used in this study. The D and G peak position of ta-DLC after annealing at 300 ºC for 60 min was found to be 1458 cm^{-1} and 1581 cum^{-1}, respectively.

Raman peak intensity also changed after annealing. D peak intensity increased from 385 counts after deposition to 804 counts after 300 ºC annealing as shown in Figure 4.2 (c). G peak intensity also increased from 620 counts to 885 counts after 300 ºC annealing as shown in Figure 4.2 (d). However, the ratio of D to G peak intensity (I_D/I_G) showed an increase from 0.580 after deposition to 0.881 and 0.910 after annealing at 300 ºC for 30 and 60 min annealing, respectively (Figure 4.2(e)).

Figure 4.2 (f) shows full width at half maximum (FWHM) of G peak as a function of annealing temperatures and times. FWHM of G peak decreased from 168 cm^{-1} after deposition to 130 cm^{-1} and 128 cm^{-1} after annealing at 300 ºC for 30 and 60 min, respectively.

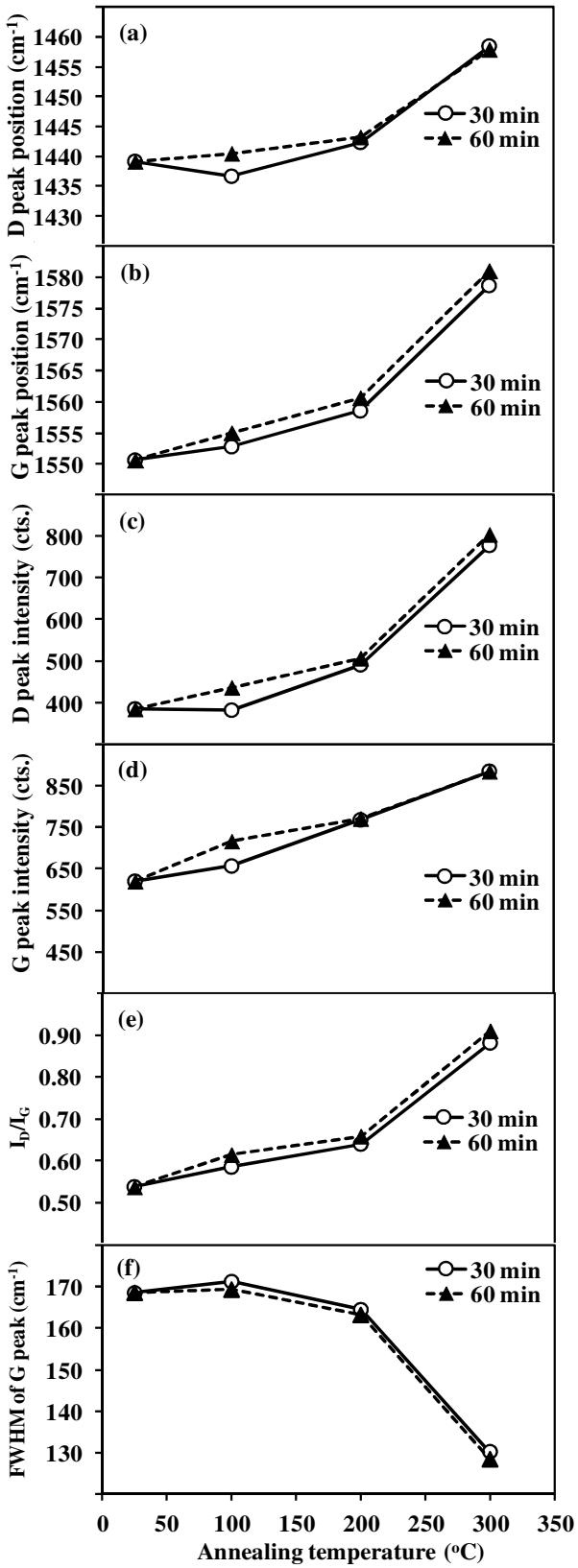

Figure 4.2 Raman parameters of the as-deposited ta-DLC and the annealed films at different temperatures and times; (a) D peak position, (b) G peak position, (c) D peak intensity, (d) G peak intensity, (e) I_D/I_G, (f) FWHM of G peak

The variation of G peak position change as a function of temperature is due to the high temperature which initially causes sp^2 clustering into fairly ordered aromatic [18-19]. Prawer et al. also suggested that an upward shift in the G peak position indicating the sp^2 carbon aggregation into larger clusters with smaller nearest neighbor distance [33]. The increase of D peak intensity also indicates an organization of sp^2 sites into nanoclusters of sp^2 rings which are formed by clustering of the sp^2 component of the film [14, 18-19, 29]. Ferrari and Robertson have verified that the width of G peak varies with disorder and used to explain about the in-plane correlation length (La) or grain size of graphite. As FWHM of G peak decreases, there is a corresponding increasing of I_D/I_G [14, 18-19].
In this study, Raman spectra were carried out at three excitation wavelengths of 514.5, 325 and 785 nm. Figure 4.3 shows the G peak position of the as-deposited ta-DLC and the annealed films at different temperatures for 60 min as function of excitation wavelength. It reveals that G peak positions decreased with increasing excitation wavelength.

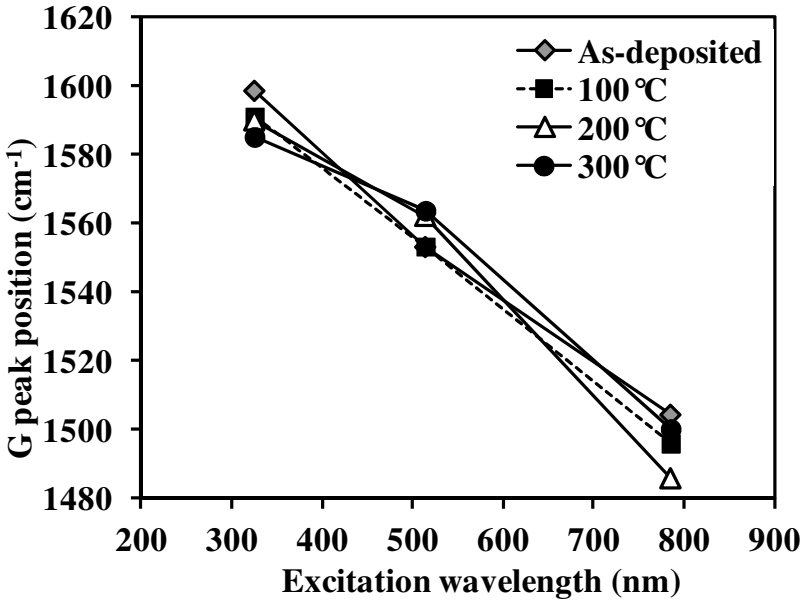

Figure 4.3 G position from multi-wavelength Raman of the as-deposited ta-DLC and the annealed films at different temperatures for 60 min.

According to Ferrari [19], the G peak only disperses in a more disordered carbon and the G peak in graphite cannot disperse because it is the Raman-active phonon mode of the crystal. This finding confirmed that the changes seen in Raman spectra of 300 ºC annealed samples in this study is not due to the sp^3 to sp^2 transformation. ta-DLC film after annealing at 300 ºC for 60 min still behaves as an amorphous carbon but with more sp^2 clustering.

4.2 Effect of thermal heating on chemical bonding

XPS was used in this study to determine the detailed bonding structure of ta-DLC after deposition and after annealing. The XPS spectra peak location or shifts reflects the chemical states as influenced by the environment of the atoms. The C1s peak position of diamond is at 285.6 eV and its FWHM is 1.45 eV. The C1s peak position and FWHM

for graphite are 284.4 eV and 1.35 eV, respectively [34]. Figure 4.4 shows the XPS C1s peak of the as-deposited ta-DLC and the annealed films at different temperatures and times. C1s core peak position shifted to higher binding energy at 300 ºC annealing. The small shoulder of C1s peak at high binding energy of 300 ºC annealed sample can be observed. This shoulder of the C1s spectrum indicated that some carbon atoms were bonded to oxygen on the ta-DLC films [34-35].

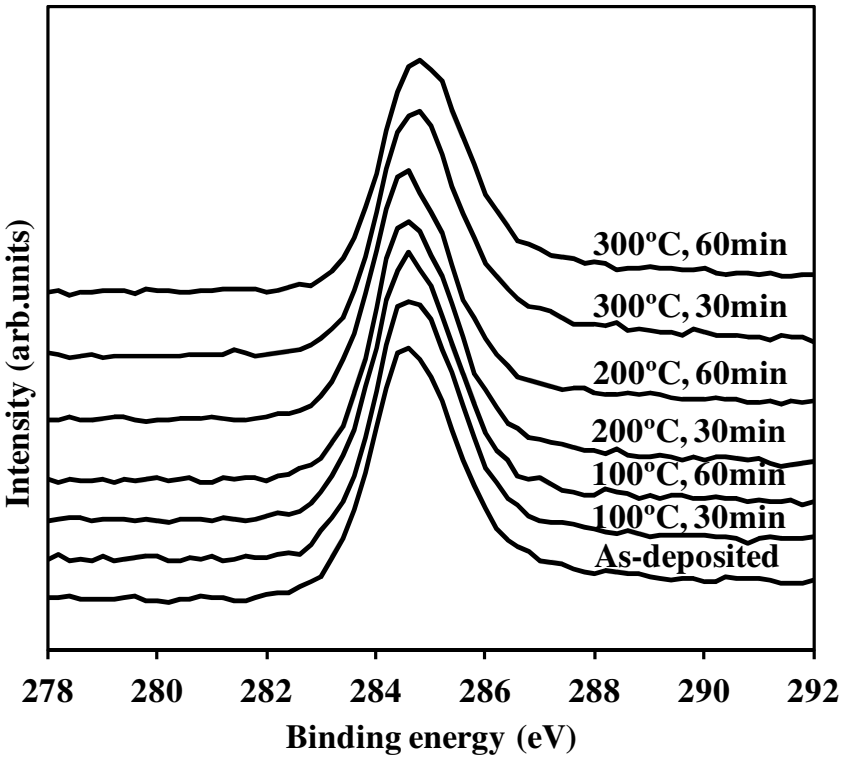

Figure 4.4 C1s spectra of the as-deposited ta-DLC and the annealed films at different temperatures and times.

The composition details of films were deduced from XPS fitting for XPS core peak both of ta-DLC and adhesion layer. The C1s and Si2p spectra were fitted with the binding energy and Gaussian width of each component. Figure 4.5 (a-b) shows the curve-fitted XPS spectra of C1s of as-deposited ta-DLC film and after annealing at 300 ºC for 60 min. The C1s spectrum in this study can be deconvoluted into five peaks located at 283.2 eV, 284.4 eV, 285.6 eV, 287.1 eV, and 288.9 eV, which are assigned to be the carbide, C-C sp^2 bond, the C-C sp^3 bond, the C-O bond, and the C=O bond or O-C=O bond, respectively [34-35].

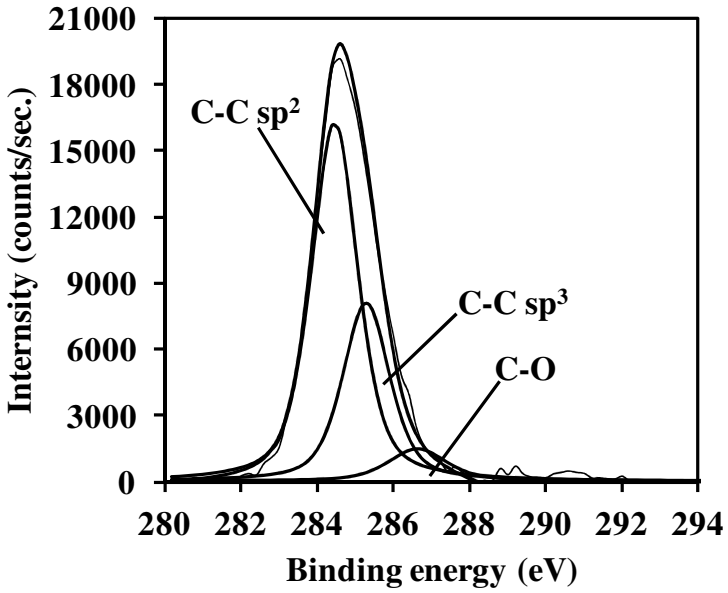

(a)

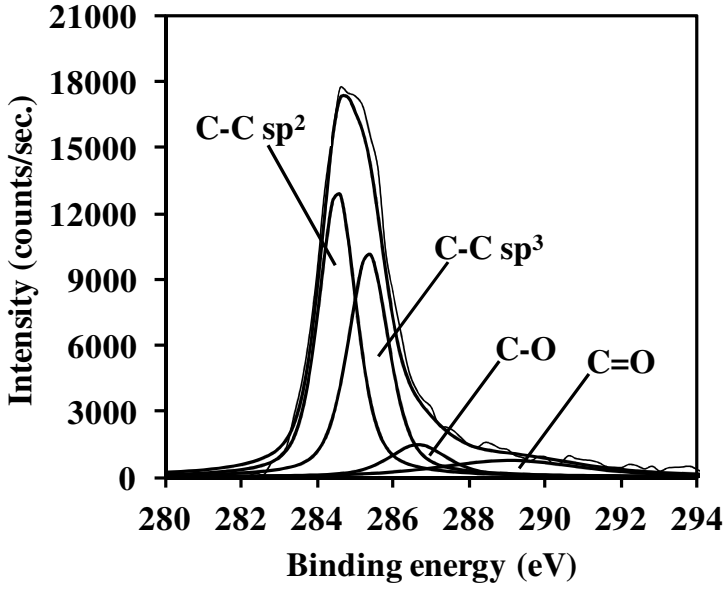

(b)

Figure 4.5 Curve-fitted XPS spectra of C1s of ta-DLC films; (a) as-deposited, (b) after annealing 300 ºC for 60 min.

The area fraction of all fitted peaks under C1s peak after heating up to 200 ºC remained the same as one after deposition. At 300 ºC, both of 30 min and 60 min annealing time, there was an increased area fraction of C-O and C=O and slightly decreasing of sp^2 bond. Sp^3 seems to be unchanged after heating up to 300 ºC. However, the observation of slightly increasing sp^3 after annealing at 300 ºC for 60 min is still not well understood. Table 4.2 shows the area fraction of all fitted peaks under C1s peak of ta-DLC as-deposited and after annealing at 300 ºC for 60 min.

Table 4.2 Area fraction of all fitted peaks under C1s peak of ta-DLC as-deposited and after annealing at 300 ºC for 60 min

Films	Carbide	Sp^2	Sp^3	C-O	C=O
As-deposited	0.00%	27.7%	61.8%	9.2%	1.3%
After annealing at 300 ºC for 60 min	0.00%	21.2%	61.5%	12.8%	4.5%

Figure 4.6 shows the Si2p peak of the adhesion layer material in the film stack after deposition after annealing. Si2p core peak position of the adhesion layer material shifted to higher binding energy site after annealing. A significant shift of Si2p core spectra to higher binding energy at 300 ºC was observed. The shoulder at lower binding energy started to disappear at 200 ºC and 60 min and has completely disappeared after 300 ºC annealing.

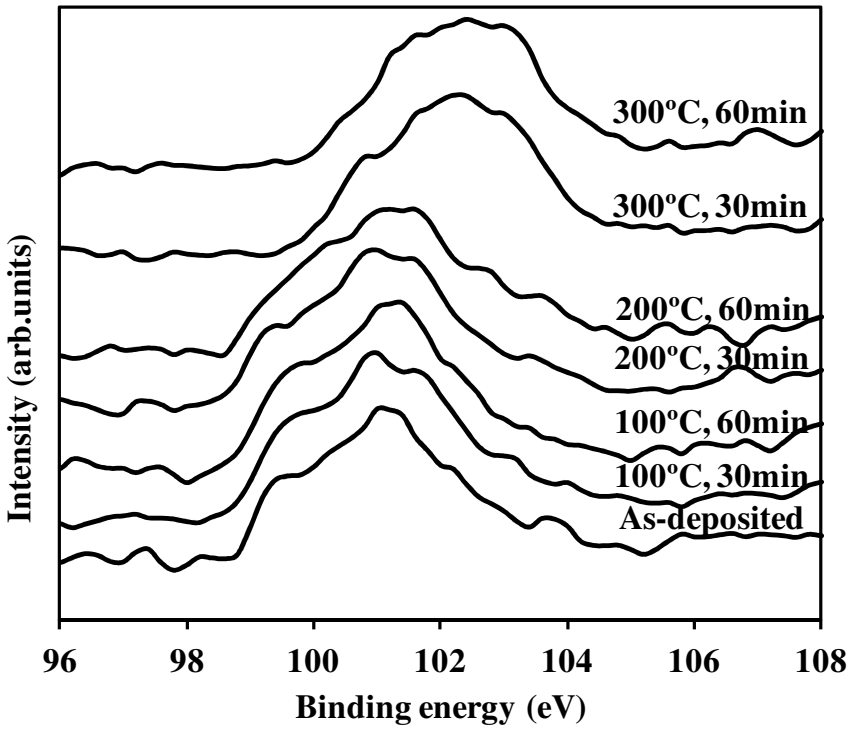

Figure 4.6 Si2p spectra of the as-deposited ta-DLC and the annealed films at different temperatures and times.

Figure 4.7 (a-b) shows the curve-fitted XPS spectra of Si2p of adhesion layer after deposition and after annealing at 300 ºC for 60 min. The Si2p spectrum in this study can be deconvoluted into five peaks located at 99-100 eV, 100.4 eV, 101.9 eV, 102.6 eV, and 103.4 eV, which are assigned to be the Si-Si bond, Si-C bond, Si-N bond, Si-O bond, and Si=O bond, respectively [36-37]. Same as Si=O, Si-C bond which normally occurred at DLC-adhesion layer interface was absent in this fitting.

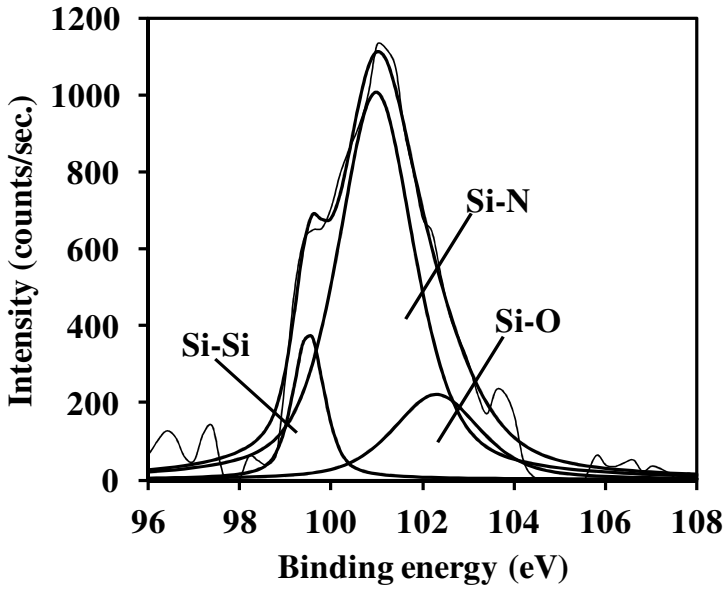

(a)

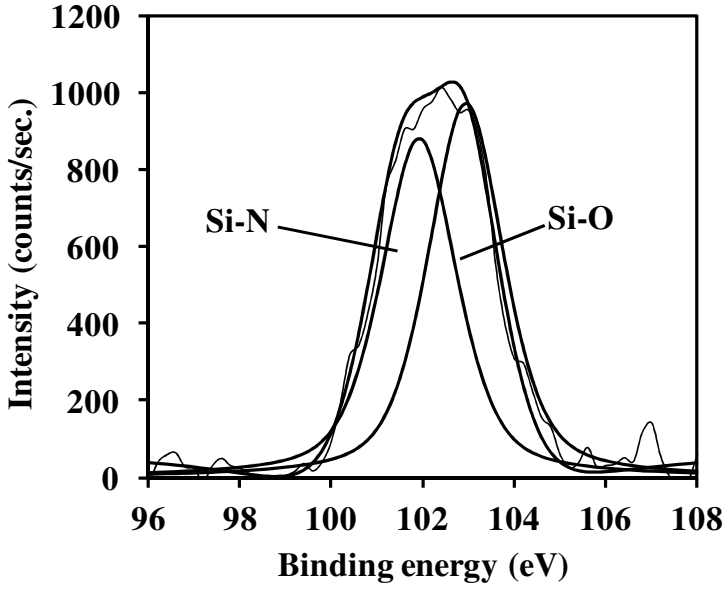

(b)

Figure 4.7 Curve-fitted XPS spectra of Si2p of ta-DLC films; (a) as-deposited, (b) after annealing 300 ºC for 60 min.

The area fraction of all fitted peaks under Si2p peak after heating up to 200 ºC and 30 min remained the same as as-deposited film. At 200 ºC with 60 min annealing can observe the Si-O bond which had started to increase. At 300 ºC, Si-Si bond completely disappeared and Si-O has significantly increased. Table 4.3 shows the area fraction of all fitted peaks under Si2p peak of ta-DLC as-deposited and after annealing at 300 ºC for 60 min.

Table 4.3 Area fraction of all fitted peaks under Si2p peak of ta-DLC as-deposited and after annealing at 300 ºC for 60 min

Films	Si-O	Si-N	Si-Si
As-deposited	11.4%	68.4%	20.2%
After annealing at 300 ºC for 60 min	53.9%	46.1%	0.0%

All information obtained from the C1s and Si2p spectra indicated that both ta-DLC films and adhesion layer were oxidized after heating up to 300 ºC.

4.3 Effect of thermal heating on wear resistance

This section presents the effect of thermal heating on film wear resistance characterized by nanoindenter.

The mechanical property of ta-DLC film was investigated by using nanoindenter to perform wear on the films. Figure 4.8 shows the wear depth of the ta-DLC films as function of annealing temperature and time. The wear depth of ta-DLC film remained constant up to 100 ºC and then increased at 200 ºC. The wear depth increased after annealing at 300 ºC for 30 min to be 0.460 nm and rapidly increased to 0.607 nm after annealing at 300 ºC for 30 min. The wear depth after annealing at 300 ºC for 60 min is close to wear depth value of substrate only which is 0.683 nm. The result obtained above suggested that the mechanical property in term of wear resistance of ta-DLC film has degraded after annealing at high temperature. Figure 4.9 shows the image of worn area after test with nanoindenter.

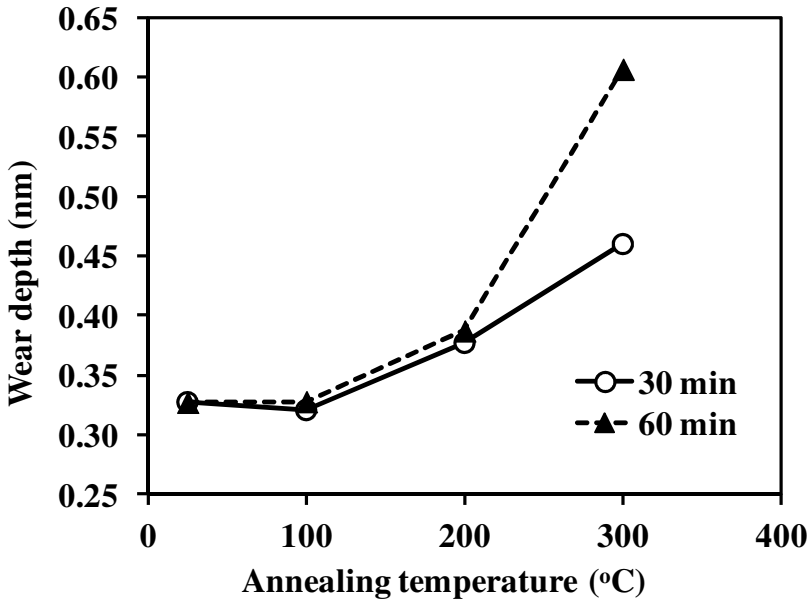

Figure 4.8 Wear depth of the as-deposited ta-DLC and the annealed films at different temperatures and times.

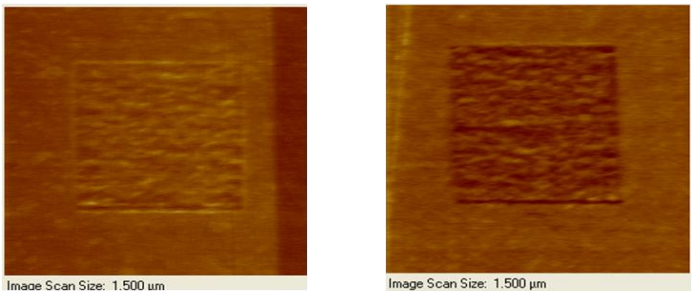

(a) (b)

Figure 4.9 Wear images of ta-DLC films; (a) as-deposited; (b) after annealing at 300 ºC for 60 min.

4.4 Effect of thermal heating on corrosion resistance

This section presents the effect of thermal heating on film corrosion resistance characterized by acid dip test.

Figure 4.10 gives the corrosion results for the DLC coated samples heated at different temperature and time. On the samples as-deposited without heating, the percent of corrosion of both groups are starting about 34-36%. At the 200 ºC, the corrosion percentage of the sample is slightly increasing as function of heating time. At the maximum of time, corrosion is about 67%. But on the 300 ºC, the percent of corrosion is monotonically increased and hit 100% corroded at 120 min.

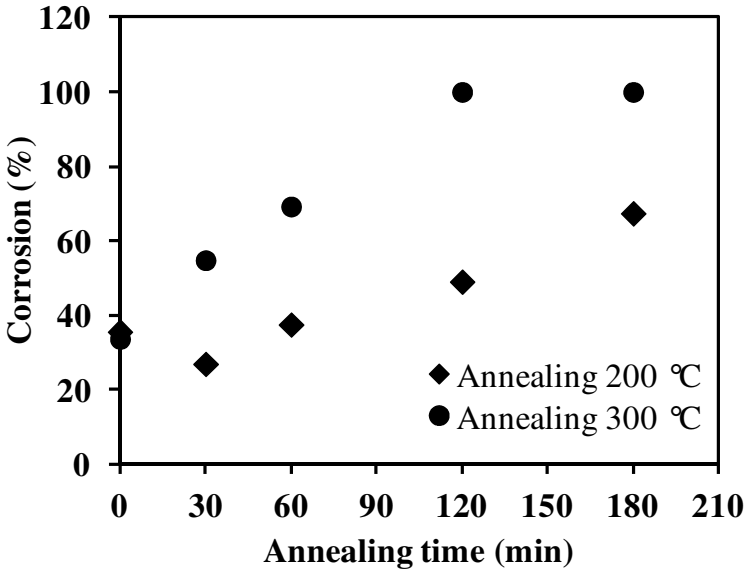

Figure 4.10 Corrosion percentage of DLC films heating at 200 ºC and 300 ºC at 0, 30, 60, 120, and 180 min

Figure 4.11 shows the defect density occurred on the samples at different heating condition compare to as-deposited. At lower heating temperature, less defect density was observed.

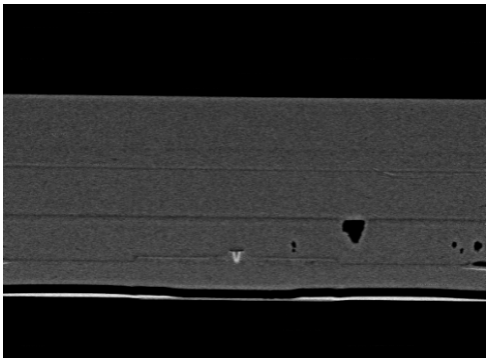

(a)

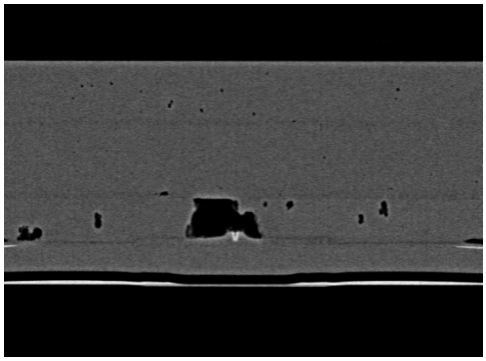

(b)

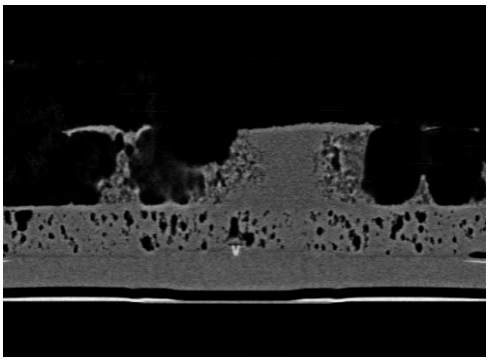

(c)

Figure 4.11 Defect density of ta-DLC films; (a) as-deposited; (b) after annealing at 200 ºC for 180 min; (c) after annealing at 300 ºC for 180 min

As structure changes observed by Raman and corrosion trend, both results can correlate to each other. The changes in corrosion percentage and Raman peaks as a function of heating suggests on the first order the increasing in the sp^2 cluster size weakens the film and led to an increase in corrosion percentage. At higher temperature such a 300 ºC, dramatically change in Raman parameter was observed which agree well on significantly worse corrosion percentage as compare to 200 ºC. The structure of DLC films in case of 300 ºC maybe different than 200 ºC condition. The other confirmation of structural analyses may be needed to fully explain this change. However, this accelerated heating test can use to accelerate corrosion percentage of sample.

4.5 Effect of thermal heating on film optical property

This section presents the effect of thermal heating on film optical property characterized by ellipsometer.

To understand more in films properties, ellipsometry was performed to measure the optical property of film after deposition and after annealing. The interested parameters in this study were reflective index (n) and extinction coefficient (k) which corresponded to the reflection and absorption properties of the films, respectively. Figure 4.12 shows the n-value and k-value of the as-deposited ta-DLC and the annealed films at different temperatures for 60 min. The n-value of ta-DLC film maintained at ~2.40 as of after deposition until after heating up to 200 ºC. After anneal at 300 ºC for 60 min, the n-value decreased to ~2.375. This information suggested that the reflection of the film tended to decrease at the temperature above 200 ºC. The k-value of ta-DLC film maintained at ~0.42 after deposition and after heating up to 100 ºC and then slightly increased to ~0.43 at 200 ºC. After anneal at 300 ºC for 60 min, k-value increased to ~0.44. This result indicated than ta-DLC film tended to absorb more light at the temperature above 100 ºC.

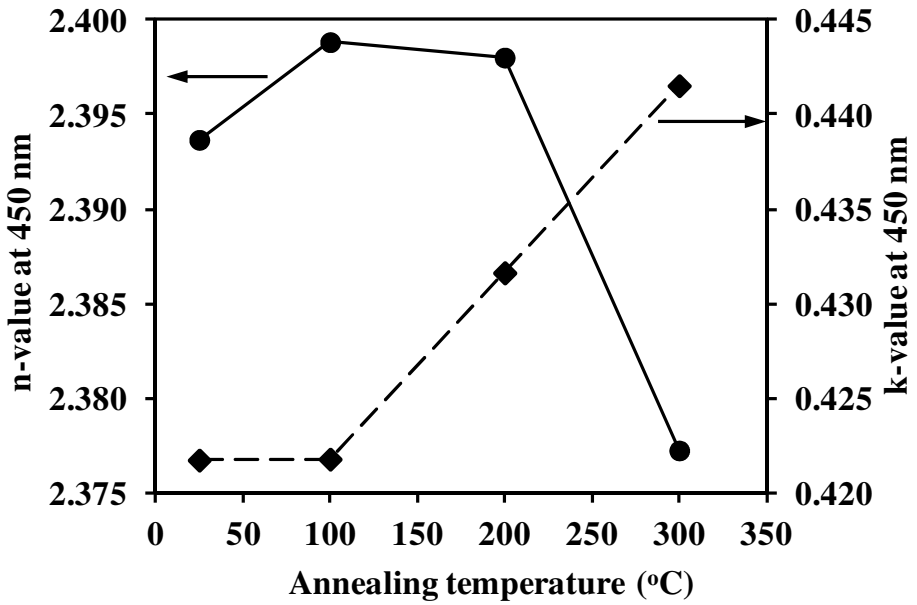

Figure 4.12 n-value and k-value of the as-deposited ta-DLC and the annealed films at different temperatures for 60 min.

4.6 Effect of thermal heating on film density

This section presents the effect of thermal heating on film density characterized by X-ray reflectivity (XRR).

To better understanding of the film property change as function of thermal heating, film density characterization using XRR was performed. After check with XRR, the result showing that there is no change of DLC film density as heating temperature increasing. Film density is still in the range of ta-C. The plot of density along heating temperature

and compare with ta-C and graphite is shown in Figure 4.13. This result agrees well with Raman which showing that there is no sp^3/sp^2 conversion at this highest temp at 300 ºC for 60 min.

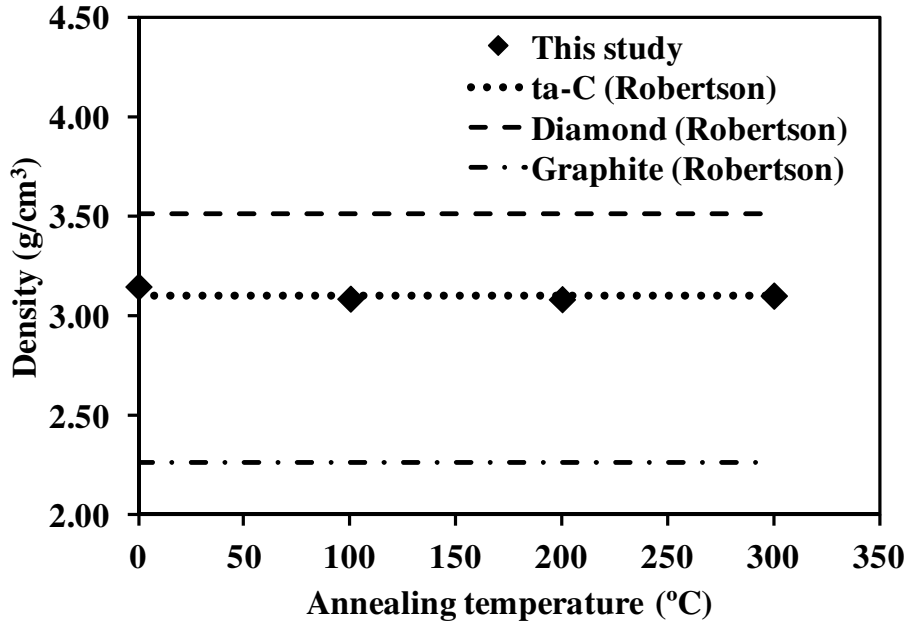

Figure 4.13 Film density of the as-deposited ta-DLC and the annealed films at different temperatures for 60 min.

4.7 Effect of thermal heating on surface roughness

This section presents the effect of thermal heating on surface roughness characterized by Atomic Force Microscopic (AFM).

To better understanding of the film property change as function of thermal heating, surface roughness characterization using AFM scanning was performed. After check with AFM, the result shows in table 4.4 that there is no change of ta-DLC film surface as heating temperature increasing. The roughness detected by AFM was dominated by substrate surface roughness which is AlTiC (alumina-titanium carbide) Figure 4.14 shows images of surface roughness of each condition.

Table 4.4 Surface roughness of as-deposited ta-DLC films and after annealing at different temperature for 60 min measured by AFM

Films	Surface roughness (Rms; nm)
ta-C as-deposited	0.315
ta-C after annealing at 100 ºC for 60 min	0.311
ta-C after annealing at 200 ºC for 60 min	0.309
ta-C after annealing at 300 ºC for 60 min	0.318

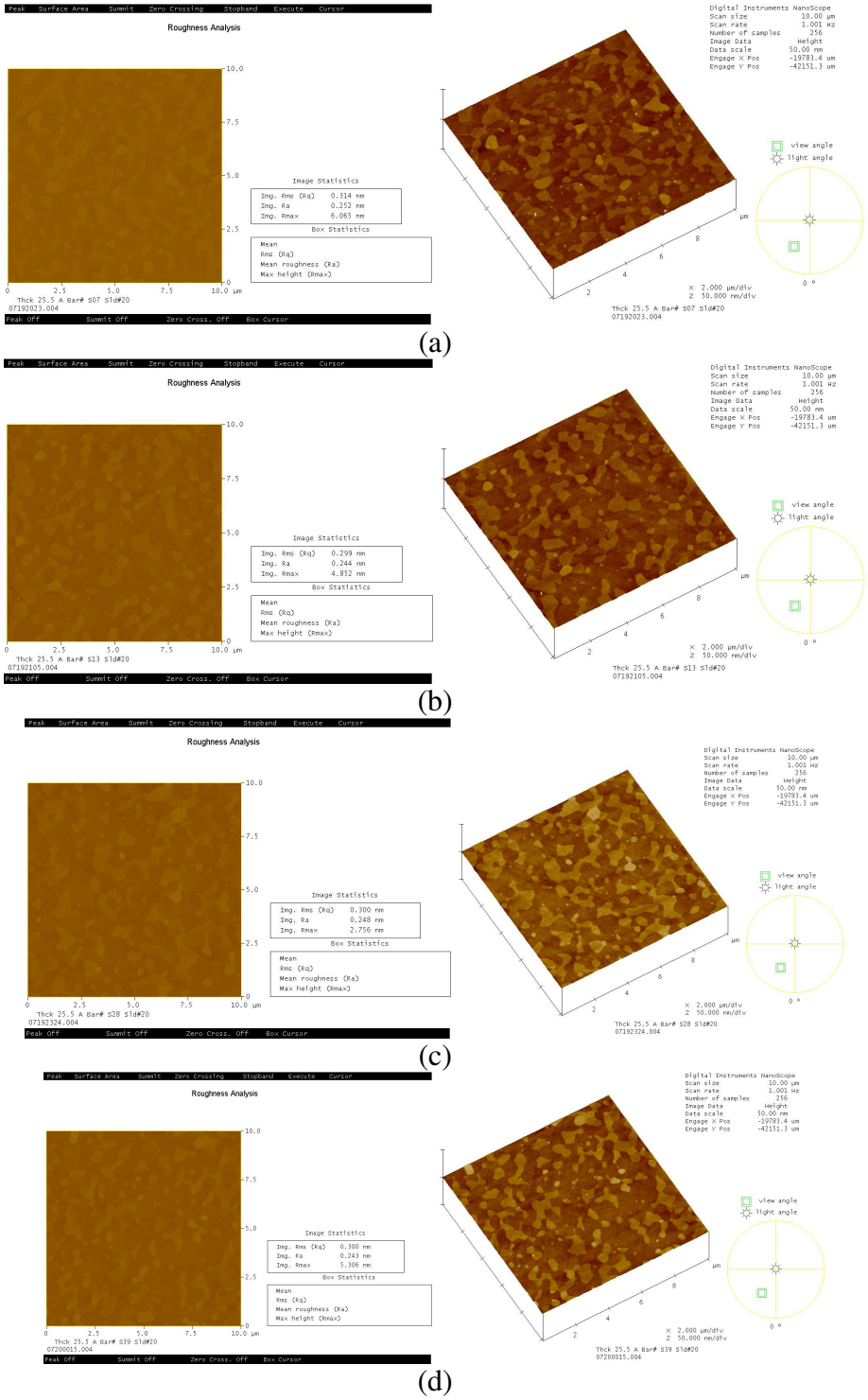

Figure 4.14 Surface roughness of ta-DLC films; (a) as-deposited; (b) after annealing 100 ºC for 60 min; (c) after annealing 200 ºC for 60 min; (d) after annealing 300 ºC for 60 min

In additional, XRR analysis also provide the surface roughness information which separate between substrate and the ta-DLC film layer. The following table 4.5 shows the surface roughness measured by XRR. The result confirms that there is no film density change along the thermal heating up to 300 ºC in this study. However, the surface roughness value measured by XRR is different from the value that measured by AFM.

Table 4.5 Surface roughness of as-deposited ta-DLC films and after annealing at different temperature for 60 min measured by XRR

Films	Surface roughness (Rms; nm)
ta-C as-deposited	0.459
ta-C after annealing at 100 ºC for 60 min	0.467
ta-C after annealing at 200 ºC for 60 min	0.455
ta-C after annealing at 300 ºC for 60 min	0.433